

## 研究成果の刊行に関する一覧表レイアウト (参考)

## 書籍

著者氏名	論文タイトル名	書籍全体の 編集者名	書 籍 名	出版社名	出版地	出版年	ページ
石坂幸人	標的ペプチドを用いた心臓難と治療法開発	(財)臨床薬理研究振興財団	臨床薬理の進歩2005	(財)臨床薬理研究振興財団	東京	2005	47-52

## 雑誌

発表者氏名	論文タイトル名	発表誌名	巻号	ページ	出版年
Nakai-Murakami C, Shimura M, Kinomoto K, Takizawa Y, Tokunaga K, Taguchi T, Hoshino S, Miyagawa K, Sata T, Kurumizaka H, Yuo A and <u>Ishizaka Y.</u>	HIV-1 Vpr induces ATM-dependent cellular signal with enhanced homologous recombination.	<i>Oncogene</i>	26	477-486	2007
Tachiwana H, Shimura M, Nakai-Murakami C, Tokunaga K, Takizawa Y, Sata T, Kurumizaka H, <u>Ishizaka Y.</u>	HIV-1 Vpr induces DNA double-strand breaks.	Cancer Res.	66	627-631	2006
Mizoguchi I, Ooe Y, Hoshino S, Shimura M, Kasahara T, Kano S, Ohta T, Takaku F, Nakayama Y, <u>Ishizaka Y.</u>	Improved gene expression in resting macrophages using an oligopeptide derived from Vpr of human immunodeficiency virus type-1.	<i>Biochem Biophys Res Commun.</i>	338	1499-506	2005
Y. Tono, C. Kojima, Y. Haba, T. Takahashi, A. Harada, S. Yagi, <u>K. Kono</u>	Thermosensitive properties of poly(amidoamine) dendrimers with peripheral phenylalanine residues	Langmuir	22	4920-4922	2006
K. Yoshino, A. Kadowaki, T. Takagishi, K. <u>Kono</u>	Temperature-sensitization of liposomes by use of N-isopropylacrylamide copolymers with varying transition endotherms	Bioconjugate Chem.	15	1102-1109	2004

<p>Saeki K, Yasugi E, Okuma E, Breit SN, Nakamura M, Toda T, Kaburagi Y, <u>Yuo A</u></p>	<p>Proteomic analysis on insulin signaling in human hematopoietic cells: identification of CLIC1 and SRp20 as novel downstream effectors of insulin</p>	<p>Am J Physiol Endocrinol Metab</p>	<p>289</p>	<p>E419-E428</p>	<p>2005</p>
<p>Nakatsu M, Doshi M, Saeki K, <u>Yuo A</u></p>	<p>Synergistic effects of dehydroepiandrosterone and retinoic acid on granulocytic differentiation of human promyelocytic NB4 cells</p>	<p>Int J Hematol</p>	<p>81</p>	<p>32-38</p>	<p>2005</p>
<p>Uchida S, <u>Yamashita K</u> 他7名、9番目</p>	<p>Binding of 14-3-3b but not 14-3-3s Controls the Cytoplasmic Localization of CDC25B: Binding Site Preferences of 14-3-3 Subtypes and the Subcellular Localization of CDC25B</p>	<p>Journal of Cell Science</p>	<p>117 (4)</p>	<p>3011-3020</p>	<p>2004</p>
<p>Mishima Y, Terui Y, Sugimura N, Matsumoto-Mishima Y, Rokudai A, Kuniyoshi R, <u>Hatake K.</u></p>	<p>Continuous treatment of bestatin induces anti-angiogenic property in endothelial cells.</p>	<p>Cancer Sci.</p>	<p>98</p>	<p>364-72.</p>	<p>2007</p>

# 標的ペプチドを用いた診断と治療法開発

石坂 幸人

臨床薬理の進歩2005別刷  
財団法人臨床薬理研究振興財団

## 標的ペプチドを用いた診断と治療法開発

Targeting of tumors detecting peptide and development of local drug delivery system

石坂 幸人<sup>\*1</sup>

Key words : 標的ペプチド、遺伝子導入、DDS、Vpr/HIV-1、Nuclear trafficking

### 背景

近年、細胞標的による新しい標的治療の可能性が明らかになりつつある。即ち、ヒト乳癌で発現するレセプター型チロシンキナーゼ、HER2遺伝子産物に対する単クローン抗体 (Herceptin)<sup>1)</sup>やEGFレセプターに対するモノクローナル抗体を用いた癌遺伝子治療<sup>2)</sup>が行われ、良好な臨床成績に加えて、担癌マウスを用いた基礎実験においても抗腫瘍効果が得られている。また、細胞標的を可能にするペプチドに対する報告も徐々に増加しており<sup>3,5)</sup>、ペプチドを用いた新しい標的治療の可能

性が期待される。私たちの研究部では、ペプチドを用いた微少癌の診断と治療法の開発を行っている。目標としているシステムを図1に示す。すなわち、種々の癌細胞を選択的に認識するペプチドを同定し、これを磁性体ナノミセルに結合させた分子とMRIを用いて癌細胞を画像化する。一方、ペプチドを結合することが可能な感温性ナノミセルを開発し、加温装置による外部照射を行うことで磁性体から発生する熱によって感温性ミセルを融解させ、ミセルに包埋した細胞形質転換因子を局所で放出させる。放出させる因子としては抗癌剤やアポトーシス誘導因子を用い、殺細胞効果を

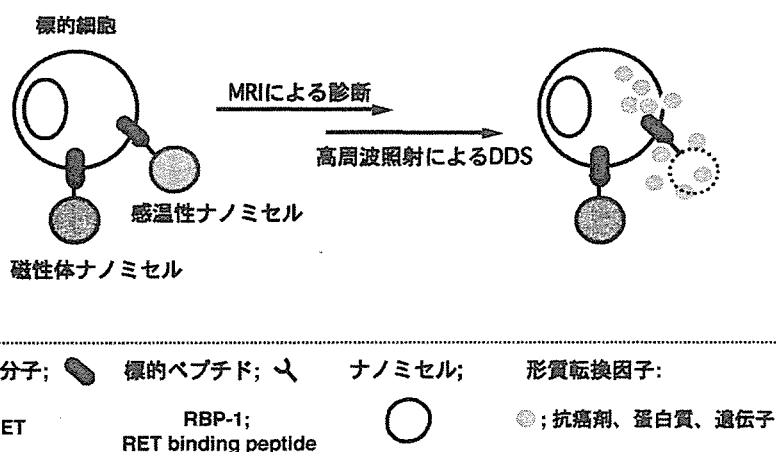


図1 ペプチドによる診断・治療法の概要

\*1 ISHIZAKA YUKIHITO 国立国際医療センター研究所

誘導する。このようなシステムにより、微小癌の早期診断が可能になるばかりでなく、局所Drug delivery system (DDS) による担癌患者QOLの改善も期待できる。

本システムを実現させるためには、様々なステップをクリアすることが必要である。すなわち、

- ① 標的分子の同定
- ② 標的分子を用いた病変部位の高感度診断法の開発
- ③ 感温性ミセルと加温装置の開発
- ④ 局所における DDSの開発

である。私の研究部の守備範囲は、1. 標的ペプチドの同定とその可能性を明らかにすることと、2. 標的細胞に対する形質転換法の開発、であり、磁性体や感温性ナノミセルを用いたシステム開発は、企業や大学との密接な連携のもとに進めている。本研究助成では、申請者が同定した細胞標的ペプチド (RET binding peptide; RBP-1) の有用性を明らかにするのに加えて、HIV遺伝子の一つであるVpr由来ペプチドを用いた新しい細胞形質転換を試みた。

RBP-1は神経芽腫細胞で高率に発現するレセプター型チロシンキナーゼ、RET<sup>6,7)</sup>の細胞外ドメインに結合性を示すペプチドで8個のアミノ酸からなる分子である。

## 1. RBP-1によるRET発現細胞に対する選択的形質転換

### a. RBP-1の同定

レセプターなどの膜抗原を認識する抗体を用いた細胞標的が可能になっている。我々もレセプター型チロシンキナーゼ、RETに対する抗体を作成し、外来遺伝子を選択的に神経芽腫細胞で発現させることに成功した<sup>8)</sup>。しかし、抗体は分子量が大きいと、磁性体やナノミセルに十分なモル比で結合させることが難しいのに加えて、生体を使用する際のエンドトキシンの問題やヒト型抗体への変換の必要性など、様々な問題点を有している。そこで、抗体からペプチド分子を用いた細胞標的の可能性を明らかにする目的で、RETに結合する8個のアミノ酸からなるペプチド、RBP-1を同定した。

RET細胞外ドメインのリコンビナント蛋白質を調整し、これに結合するペプチドをランダムペプチドディスプレイライブラリー (RPDL; random peptide display library) (図2) から同定した。RPDL (インビトロジェン社) は約 $10^9-10^{10}$ 個のバクテリアのプールからなっており、それぞれのバクテリアが12個のアミノ酸がランダムに並ぶペプチドを一つ発現している。RETのリコンビナント蛋白質をプレートにコートした後、RPDLを作用さ

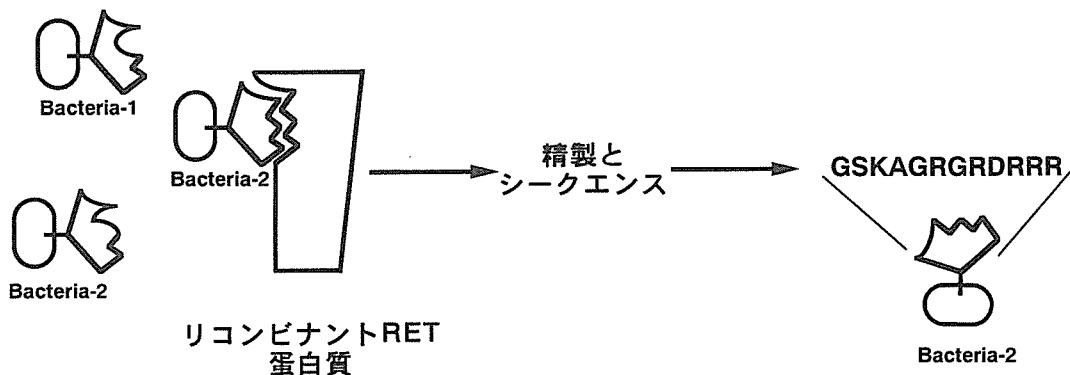


図2 ランダムペプチドディスプレイライブラリーの概要

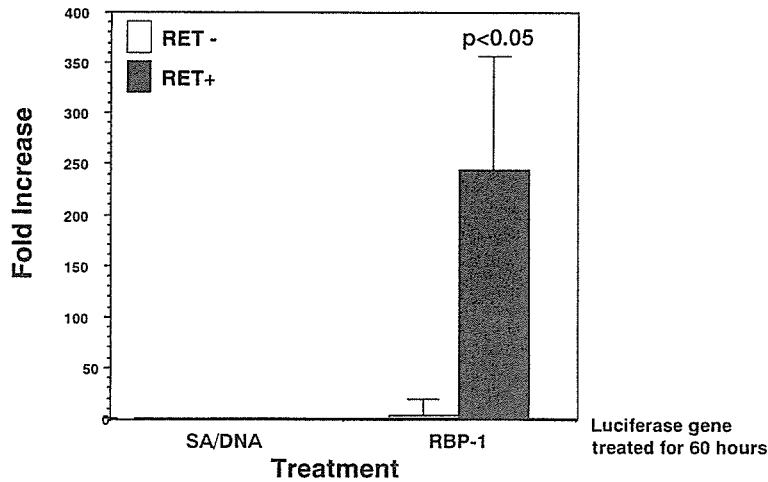


図3 RBP-1を用いた選択的遺伝子導入

ビオチン化したりポータープラスミドDNAをストレプトアビジン、ビオチン化RBP-1とともに細胞へ作用させた。導入60時間後にルシフェラーゼ活性を測定した。各検体について3つずつ作成し、平均値と標準偏差（エラー・バー）を算出して、表記した。

せ、蛋白質に結合するバクテリアを回収した。このパニングを5回繰り返した後、得られたバクテリア中のプラスミドDNAのシーケンスを行い、予測されるアミノ酸配列を比較した。その結果、グリシン (G) およびアルギニン (R) からなるモチーフがコアになっていることが示唆された。そこで、得られたクローンの代表として、KAGRGRDRの配列を有するペプチド (RBP-1) を合成し、RET分子に対する結合性を解析した。

#### b. RBP-1のRET発現細胞への結合と選択的遺伝子導入

RET発現細胞として神経芽腫細胞株 (NB-39-nu)、RET非発現細胞としてヒト線維肉腫細胞株 (HT1080) を用いて、RBP-1の結合性を検定した。N-末端をビオチン化したRBP-1を種々の濃度で培養系に添加し、一晚作用させた後、FITC標識ストレプトアビジン (以下SA-FITC) を用いて、ペプチドを検出した。その結果、RBP-1は神経芽腫細胞に選択的に結合し、胞体内に取り込まれることが示唆された。

次にビオチン化RBP-1とアビジン化ポリリジンおよび、プラスミドDNAを用いて選択的な遺伝子導入発現の可能性を解析した。その結果、RET発現細胞では、コントロール細胞と比較して、数十倍の外来遺伝子発現の上昇が検出された (図3)。

以上の結果は、このペプチドが細胞標的を可能にするきわめて有用なペプチドであることを意味するとともに、細胞標的が数個のアミノ酸からなるペプチドを用いても可能になることを示唆する。現在、このペプチドと磁性体との結合様式を検討しており、標的細胞のMRIによる撮像を行うべく準備中である。

#### c. 今後の展開

RETは神経芽腫に比較的選択的に発現している。本システムを一般化するためには、癌組織で普遍的に発現する分子を認識するペプチドの開発が重要である。近年、腫瘍細胞が増殖するのに必要な血管内皮細胞の増殖が血管内皮細胞増殖因子受容体 (KDR-1/VEGFR) を介していることが示され、この分子が格好の標的分子になる可能性が

示された<sup>9)</sup>。そして、KDR-1に結合するペプチドも同定されている<sup>10)</sup>。我々もKDR-1標的ペプチドを用いた標的化を検討中である。また、種々の臓器由来細胞に選択性を示すペプチドのライブラリーを準備することも必要である。

## 2. 標的細胞の核へのトラフィッキングを可能にする分子の同定

標的細胞に対して、効率良く形質転換を誘導するシステムの開発は、本プロジェクトを達成する上で重要である。現在、形質転換効率の高いシステムとしてアデノウイルスが使用されているが、我々は非ウイルス性ベクターシステムの開発を目指している。当研究部ではHIV-1の研究を平行して行っており、中でもアクセサリ遺伝子の一つであるVprを中心に解析を進めている<sup>11)</sup>。Vprは形質転換ベクターとして機能する可能性のある興味深い分子である。即ち、Vprを細胞の培養液中に添加すると速やかに胞体内に取り込まれることが報告されている<sup>12)</sup>。このような機能は同じHIV-1遺伝子であるTatについても認められており、これまでに様々な形でTatの形質転換ベクターとしての可能性が示されている<sup>13)</sup>。そこで、Vprが細胞

内に取り込まれるために必要な最小領域を明らかにする一方、これを用いた細胞形質転換を試みた。

### a. 最小機能ドメインの同定

Vprは96個のアミノ酸からなる蛋白質で、C-末端45個のアミノ酸からなるペプチド(C45)にも、胞体内に取り込まれる機能が報告されていた<sup>14)</sup>。しかし、Vprは細胞周期異常を強力に誘発するだけでなく、染色体分離異常も誘発することを見出した(文献-11)。即ち、C-末端を有するペプチドは、正常細胞に対して致命的な欠陥を有していることが示唆された。そこで、活性を保有しながら細胞周期に影響を示さない領域を同定することを試みた。以前の解析では、C-末端18個のアミノ酸を欠失した変異型Vprには細胞周期異常を誘発する活性が認められなかった<sup>14)</sup>。そこで、C45からC末端18個のアミノ酸を欠失させたペプチド(以下C45D18)の機能を解析した。N-末端にビオチンを付加したペプチドを細胞の培養液中に添加し、一晩培養した後、SA-FITCを用いて検出した。その結果、HT1080細胞およびヒト臍帯血由来単核球細胞ともにほぼ100%の頻度でペプチドが取り込まれていることが判明した(図4)。

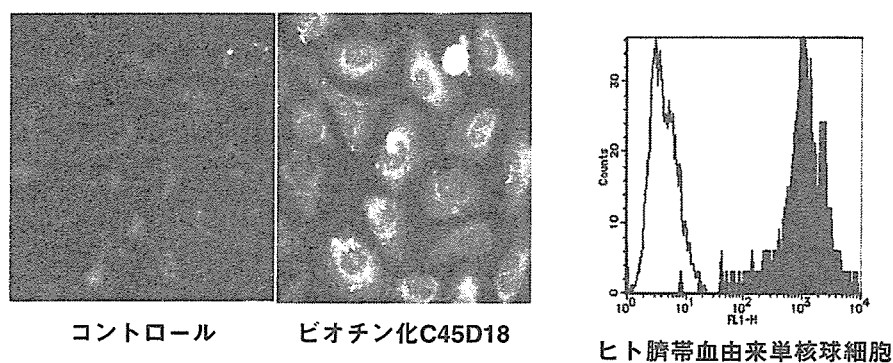


図4 C45D18の胞体内への取込

ビオチン化したC45D18をHT1080細胞とヒト臍帯血由来単核球細胞に一晩作用させ、FITC-SAで検出した。左は染色像、右はFACSによる解析の結果を示す。図中右側に位置するピーク(右のパネル)がペプチドを取り込んだ細胞集団で、ほぼ全ての細胞にペプチドが取り込まれている。

#### b. 最小ペプチドを用いたリコンビナント蛋白質の核内へのトラフィッキング

C45D18の機能を用いて、細胞外から胞体内への蛋白質のトラフィッキングを試みた<sup>15)</sup>。まず、ペプチドを種々のモル比でリコンビナント蛋白質であるGreen fluorescence protein (以下GFP) に結合させ、培養液に添加すると結合させたモル比に応じて、胞体内に取り込まれるGFP陽性細胞の頻度が上昇した。興味深いことに、胞体内に取り込まれたGFPは、核染に一致して検出された。また共焦点レーザー顕微鏡を用いた解析でも、取り込まれたGFPは核の局在と一致したことから、C45D18が細胞外から核内にリコンビナント蛋白質を運搬する機能を有していることが示された。

#### c. 非分裂細胞へのリコンビナント蛋白質の導入

HIV-1はレトロウイルスの一種であるが、他のウイルスと決定的に異なる特性として、分裂していない細胞にも感染できる。Vprは、静止期にあるマクロファージ系細胞へのウイルス感染に必須であることが知られている。そこで、C45D18のトラフィッキング機能が非分裂細胞に対しても示す可能性を考え、以下の実験を行った。即ち、DNAポリメラーゼの阻害剤であるアフィデイコリン (APC) を用いて強制的に細胞周期を停止させた細胞に、C45D18を付加したGFPを投与した。その結果、コントロール群 (無処理の細胞およびAPCの溶媒として用いてDMSO添加群) と同様にAPCを処理した細胞群でもGFPの取り込みが同程度に認められた。この際、BrdUの取り込みを観

察すると、APC添加群でDNA合成が著明に低下していることが示された。

一方、C45D18を作用させた後の細胞周期を解析すると異常は検出されなかった<sup>15)</sup>。

### 3. 考察

本研究で、ペプチドを用いた細胞標的の可能性と細胞の外から胞体内、特に核へのトラフィッキングシステムの実現性が明らかになった。このようなシステムは例えば、感温性ミセルから放出した蛋白質や遺伝子を核内に直接運搬するための良いツールになると考えている。これまでに、C45D18を用いて非分裂細胞に対する遺伝子発現を試みている。しかし、C45D18をプラスミドDNAと直接結合させた場合には有意な遺伝子発現誘導は認めなかった。現在、ポリエチルイミン (PEI) などのカチオニックリピッドにC45D18を結合させた分子を用いて、遺伝子発現誘導の有無を検討している。一般的にPEIなどのカチオニックリピッドによる遺伝子導入はエンドゾームを介しており、非分裂細胞に対する遺伝子発現は期待できない。C45D18を付加することで、遺伝子を直接核内へ運搬できれば、静止細胞でも遺伝子導入発現が誘導されるものと期待される。

### 4. 謝辞

本研究の一部は、臨床薬理研究振興財団の助成によった。自由な発想で実験を行うことができる機会を与えて頂き、深謝致します。



## 文 献

- 1) Katsumata M, Okudaira T, Samanta A, et al. Prevention of breast tumour development in vivo by downregulation of the p185neu receptor. *Nat Med* 1995; **7**: 644-648.
- 2) Chen J, Gamous S, Takayanagi A, et al. Targeted in vivo delivery of therapeutic gene into experimental squamous cell carcinomas using anti-epidermal growth factor receptor antibody: immunogene approach. *Hum Gene Ther* 1998; **9**: 2673-2681.
- 3) Park B-W, Zhang H-T, Wu C, et al. Rationally designed anti-HER2/neu peptide mimetic disables p185HER/neu tyrosine kinases in vitro and in vivo. *Nat Biotech* 2000; **18**: 194-198.
- 4) Niclin SA, White SJ, Watkins SJ, et al. Selective targeting of gene transfer to vascular endothelial cells by use of peptides isolated by phage display. *Circulation* 2000; **102**: 231-237.
- 5) Jost PJ, Harbottle RP, Knight A, et al. A novel peptide, THALWHT, for the targeting of human airway epithelia. *FEBS Lett* 2001; **489**: 263-269.
- 6) Ikeda I, Ishizaka Y, Tahira T, et al. Specific expression of the ret proto-oncogene in human neuroblastoma cell lines. *Oncogene* 1990; **5**: 1291-1296.
- 7) Takahashi M, Buma Y, Taniguchi M. Identification of the ret proto-oncogene product in neuroblastoma and leukemic cells. *Oncogene* 1991; **6**: 297-301.
- 8) Yano L, Shimura M, Taniguchi M, et al. Improved gene transfer to neuroblastoma cells by a monoclonal antibody targeting RET, a receptor tyrosine kinase. *Hum Gene Ther* 2000; **11**: 995-1004.
- 9) Niethammer AG, Xiang R, Becker JC, et al. A DNA vaccine against VEGF receptor 2 prevents effective angiogenesis and inhibits tumor growth. *Nat Med* 2002; **12**: 1369-1375.
- 10) Hetian L, Ping A, Shumei S, et al. A novel peptide isolated from a phage display library inhibits tumor growth and metastasis by blocking the binding of vascular endothelial growth factor to its kinase domain receptor. *J Biol Chem* 2002; **277**: 43137-43142.
- 11) Shimura M, Tanaka Y, Nakamura S, et al. Micronuclei formation and aneuploidy induced by Vpr, an accessory gene of human immunodeficiency virus type 1. *FASEB J* 1999; **13**: 621-637.
- 12) Sherman MP, Schubert U, Williams SA, et al. HIV-1 Vpr displays natural protein-transducing properties: implication for viral pathogenesis. *Virology* 2002; **302**: 95-105.
- 13) Fawell S, Seery J, Daikh Y, et al. Tat-mediated delivery of heterologous proteins into cells. *Proc Natl Acad Sci USA* 1994; **91**: 664-668.
- 14) Kichler A, Pages J-C, Leborgne C, et al. Efficient DNA transfection mediated by the C-terminal domain of human immunodeficiency virus type 1 viral protein R. *J Virol* 2000; **74**: 5424-5431.
- 15) Taguchi T, Shimura M, Osawa Y, et al. Nuclear trafficking of macromolecules by an oligonucleotide derived from Vpr of human immunodeficiency virus type 1. *Biochem Biophys Res Commun.* 2004; **320**: 18-26.

# HIV-1 Vpr Induces DNA Double-Strand Breaks

Hiroaki Tachiwana,<sup>1,2</sup> Mari Shimura,<sup>2</sup> Chikako Nakai-Murakami,<sup>2</sup>  
Kenzo Tokunaga,<sup>3</sup> Yoshimasa Takizawa,<sup>1,2</sup> Tetsutaro Sata,<sup>3</sup>  
Hitoshi Kurumizaka,<sup>1</sup> and Yukihito Ishizaka<sup>2</sup>

<sup>1</sup>Graduate School of Science and Engineering, Waseda University; <sup>2</sup>Department of Intractable Diseases, International Medical Center of Japan; and <sup>3</sup>Department of Pathology, National Institute of Infectious Diseases, Tokyo, Japan

## Abstract

Recent observations imply that HIV-1 infection induces chromosomal DNA damage responses. However, the precise molecular mechanism and biological relevance are not fully understood. Here, we report that HIV-1 infection causes double-strand breaks in chromosomal DNA. We further found that Vpr, an accessory gene product of HIV-1, is a major factor responsible for HIV-1-induced double-strand breaks. The purified Vpr protein promotes double-strand breaks when incubated with isolated nuclei, although it does not exhibit endonuclease activity *in vitro*. A carboxyl-terminally truncated Vpr mutant that is defective in DNA-binding activity is less capable of Vpr-dependent double-strand break formation in isolated nuclei. The data suggest that double-strand breaks induced by Vpr depend on its DNA-binding activity and that Vpr may recruit unknown nuclear factor(s) with positive endonuclease activity to chromosomal DNA. This is the first direct evidence that Vpr induces double-strand breaks in HIV-1-infected cells. We discuss the possible roles of Vpr-induced DNA damage in HIV-1 infection and the involvement of Vpr in further acquired immunodeficiency syndrome-related tumor development. (Cancer Res 2006; 66(2): 627-31)

## Introduction

A high incidence of malignant tumors, such as non-Hodgkin's lymphoma, Kaposi's sarcoma, and invasive cervical cancer [acquired immunodeficiency syndrome (AIDS)-defining cancers], is epidemiologically associated with HIV-1 infection (1, 2). These neoplasms are attributable mainly to diseases that accompany immunodeficiency, including coinfection with EBV, human herpes virus 8, and human papillomavirus (1, 2). In addition to these AIDS-defining cancers, several non-AIDS-defining cancers also occur with a higher incidence in HIV-infected individuals (3, 4). These reports lead to the assumption that HIV-1 has the potential to induce neoplasms before AIDS develops. Recently, DNA damage responses have been observed in precancerous lesion before inactivation of p53 (5, 6). Interestingly, it has been reported that HIV-1 infection induces DNA damage responses by activating Rad3-related or ataxia-telangiectasia mutated proteins and pro-

moting phosphorylation of their downstream substrates (7, 8). The elucidation of the factor triggering the DNA damage responses to HIV-1 infection is essential to determine the as yet unknown mechanism causing AIDS-related neoplasms. In the present study, we found that HIV-1 infection induces double-strand breaks of chromosomal DNA, as detected using pulsed-field gel electrophoresis (PFGE). We further showed that *vpr*, an accessory gene of HIV-1 encoding a virion-associated nuclear protein, which induces cell cycle accumulation at G<sub>2</sub>-M phase and increases ploidy (9), was a factor responsible for double-strand breaks. We discuss the potential ability of Vpr-induced double-strand breaks to develop into neoplasms in HIV-1 infection.

## Materials and Methods

**Cell culture.** MIT-23 and ΔVpr, a mock transfectant, were established from HT1080 (JCRB9113; the Health Science Research Resources Bank) as previously described (9). In MIT-23, Vpr expression is controlled by the *rtet* promoter on incubation with 3 μg/mL doxycycline (Sigma, St. Louis, MO) for 48 hours.

**Virus infection.** Vesicular stomatitis virus G protein (VSV-G)-pseudotyped HIV-1 was produced by cotransfection with a plasmid encoding VSV-G (pHIT/G) and the pNL-Luc-E<sup>+</sup>R<sup>+</sup> or pNL-Luc-E<sup>-</sup>R<sup>-</sup> proviral clone (10). (10). The preparation and titration of viruses are described elsewhere (11). Briefly, the concentration of p24 antigen in the culture supernatant was measured using a p24 Gag antigen capture ELISA kit (ZeptoMetrix, Buffalo, NY). The infectivity of the prepared viral stock was examined using MAGIC5 cells. HT1080 cells were infected for 48 hours with viruses that had 200 ng/mL of p24 Gag antigen, giving a multiplicity of infection (MOI) of 0.7.

**Immunostaining.** Immunostaining was carried out as described (9). A rabbit polyclonal Rad51 antibody raised against the bacterially expressed protein and a mouse monoclonal antibody raised against synthesized peptides of full-length of Vpr (mAb8D1) were used as the primary antibody. Goat anti-rabbit IgG conjugated with Alexa Fluor 488 (Molecular Probes, Inc., Eugene, OR) and goat anti-mouse IgG conjugated with Cy3 (Zymed Laboratories, Inc., San Francisco, CA) were used as the secondary antibodies. Images were captured on a phase contrast microscope, BX50 (Olympus Corp., Tokyo Japan), or a Radiance 2100 laser scanning confocal microscope (Carl Zeiss, Oberkochen, Germany).

**Overexpression and purification of Vpr and its mutant.** The HIV-1 *vpr* gene was ligated into the *Nde*I and *Bam*HI sites of the pET15b vector (Novagen, Madison, WI). The Vpr protein and VprΔC12 mutant were produced in the *Escherichia coli* BL21 (DE3) Codon(+)RIL strain (Novagen) by induction with isopropyl-β-D-thiogalactopyranoside (IPTG; Nacalai Tesque, Inc., Kyoto, Japan) and were purified as described in Supplementary Method. The concentration of the purified Vpr protein was determined with a Bio-Rad protein assay kit (Bio-Rad Laboratories, Hercules, CA) using bovine serum albumin (BSA) as the standard.

**Isolation of nuclei.** Cells scraped from culture dishes were washed once with ice-cold PBS and resuspended in 3 mL of ice-cold 20 mmol/L Tris-HCl buffer (pH 7.6) containing 60 mmol/L KCl, 15 mmol/L NaCl, 5 mmol/L MgCl<sub>2</sub>, 1 mmol/L DTT, 250 mmol/L sucrose, 0.6% NP40, and

Note: Supplementary data for this article are available at Cancer Research Online (<http://cancerres.aacrjournals.org/>).

Requests for reprints: Hitoshi Kurumizaka, Graduate School of Science and Engineering, Waseda University, 3-4-1 Okubo, Shinjuku-ku, 169-8555 Tokyo, Japan. Phone: 81-3-5286-8189; Fax: 81-3-5292-9211; E-mail: kurumizaka@waseda.jp and Yukihito Ishizaka, Department of Intractable Diseases, International Medical Center of Japan, 1-21-1 Toyama, Shinjuku-ku, 162-8655 Tokyo, Japan. Phone: 81-3-5272-7527; E-mail: zakay@ri.imcj.go.jp.

©2006 American Association for Cancer Research.

doi:10.1158/0008-5472.CAN-05-3144

protease inhibitor mixture (Sigma). The cell suspension was incubated for 10 minutes on ice and the sucrose concentration was adjusted to 1.6 mol/L. Then, the sample was loaded onto a sucrose cushion of 2.3 mol/L sucrose solution and centrifuged at  $35,000 \times g$  for 30 minutes. The isolated nuclei were obtained in the 2.3 mol/L sucrose fraction. For immunostaining, isolated nuclei were cytocentrifuged to the MAS-coated slide glass (Matsunami Glass IND., LTD., Tokyo, Japan) for 6 minutes at 800 rpm (Thermo Shandon, Chadwick Road, United Kingdom).

**PFGE assay.** Isolated nuclei were incubated with 10  $\mu\text{mol/L}$  of purified Vpr or Vpr $\Delta\text{C12}$  for 15 hours at 30°C. The cells (isolated nuclei) were embedded in agarose plugs at a density of  $3 \times 10^5$  cells/100  $\mu\text{L}$ . The plugs were treated with proteinase K solution [0.5 mol/L EDTA (pH 8.0), 1% sarcosyl, and 0.5 mg/mL proteinase K] for 38 hours at 50°C. After PFGE was done in a CHEFF Mapper (Bio-Rad Laboratories), the gels were stained with Vistra Green (Amersham Bioscience, Piscataway, NJ).

**The DNA-binding assay.** The Vpr protein was incubated with  $\phi\text{X174}$  single-stranded DNA (ssDNA; 20  $\mu\text{mol/L}$ ) or  $\phi\text{X174}$  superhelical dsDNA (10  $\mu\text{mol/L}$ ) in 10  $\mu\text{L}$  of 8 mmol/L Tris-HCl buffer (pH 8.5) containing 1 mmol/L DTT and 100  $\mu\text{g/mL}$  BSA. The reaction mixtures were incubated for 1 hour at 37°C and were analyzed by electrophoresis on a 0.8% agarose gel in  $1 \times$  TAE buffer (40 mmol/L Tris acetate and 1 mmol/L EDTA) at 3.3 V/cm for 2 hours. The bands were visualized using ethidium bromide staining.

**Nuclease activity.** The Vpr protein (18.8  $\mu\text{mol/L}$ ) or DNaseI (Invitrogen Corporation, Carlsbad, CA; 0.02 unit/ $\mu\text{L}$ ) were incubated with  $\phi\text{X174}$  superhelical double-stranded DNA (dsDNA; 2.5  $\mu\text{mol/L}$ ) in 40  $\mu\text{L}$  of 15 mmol/L Tris-HCl buffer (pH 8.5) containing 1 mmol/L DTT and 100  $\mu\text{g/mL}$  BSA, in the presence of 5 mmol/L  $\text{MgCl}_2$ ,  $\text{MnCl}_2$ ,  $\text{ZnSO}_4$ , or  $\text{CaCl}_2$ . The reaction mixtures were incubated at 37°C for 30 minutes. After incubation, the samples were treated with proteinase K (0.3 mg/mL) in the presence of 0.1% SDS and the DNA was extracted using phenol-chloroform. The DNA was precipitated by ethanol and was analyzed by electrophoresis on a 0.8% agarose gel in  $1 \times$  TAE buffer at 6.6 V/cm for 30 minutes. The bands were visualized with ethidium bromide staining.

**The Ni-NTA agarose pull-down assay.** Isolated nuclei were disrupted in 20 mmol/L Tris-HCl buffer (pH 8.5) containing 200 mmol/L KCl, 2 mmol/L 2-mercaptoethanol, 0.25 mmol/L EDTA, and 10% glycerol. The extract was incubated with His<sub>6</sub>-Vpr (53  $\mu\text{mol/L}$ ) for 15 hours at 30°C. After incubation, His<sub>6</sub>-Vpr was precipitated with 4  $\mu\text{L}$  of Ni-NTA agarose beads and the beads were washed thrice with 500  $\mu\text{L}$  of 20 mmol/L Tris-HCl buffer (pH 7.6) containing 100 mmol/L NaCl, 5 mmol/L DTT, 10 mmol/L imidazole, 1 mmol/L EDTA, and 0.2% Tween 20. The proteins precipitated with the Ni-NTA beads were analyzed by 16% SDS-PAGE. The bands were visualized by silver staining.

## Results

### Vpr expression induces chromosomal double-strand breaks.

To test whether HIV-1 infection causes double-strand breaks, we used PFGE, which was able to clearly detect the double-strand breaks induced by X-ray irradiation (Fig. 1A, lane 2; ref. 12). HT1080 cells were infected with HIV-1 that had 200 ng/mL of p24 Gag antigen, giving a MOI of 0.7, and the cellular DNA was fractionated using PFGE. Figure 1A (lane 6) shows that HIV-1 infection induced double-strand breaks. Interestingly, the amount of HIV-1-dependent double-strand breaks was reduced significantly (Fig. 1A, lane 5) when the *vpr* gene was deleted from the HIV-1 viral genome (HIV-1 $\Delta\text{Vpr}$ ). To show that HIV-1-dependent double-strand breaks are attributable to Vpr expression, we examined double-strand break formation in Vpr stable transfectant, MIT-23 (9), in which Vpr expression is controlled by the *rtet* promoter by doxycycline, and, in  $\Delta\text{Vpr}$ , a mock transfectant. As shown in Fig. 1B, double-strand breaks were observed in the Vpr-expressing cells (lane 5, arrow) but not in the mock transfectants (lane 4). Furthermore, Rad51 foci, which are formed

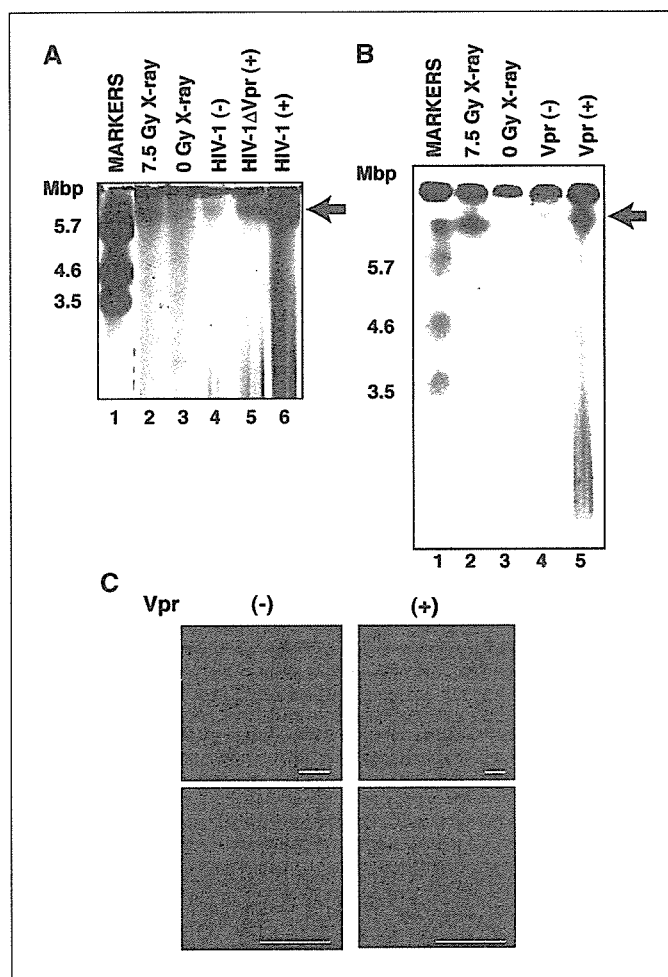


**Figure 1.** Vpr induces double-strand breaks *in vivo*. **A**, PFGE analysis of double-strand breaks after HIV-1 infection. HT1080 cells were infected with the same amount of HIV-1 or HIV-1 $\Delta\text{Vpr}$  (MOI = 0.7) and subjected to PFGE. As a positive control, uninfected cells were analyzed immediately after 7.5 Gy of X-ray irradiation. Molecular mass markers (lane 1), control cells (lanes 3 and 4), cells subjected to X-ray irradiation (lane 2), and cells infected with HIV-1 $\Delta\text{Vpr}$  (lane 5) or HIV-1 (lane 6) are shown. Arrow, position corresponding to the double-strand breaks. **B**, PFGE analysis in Vpr-expressing cells. Molecular mass markers (lane 1), cells irradiated with 7.5 Gy (lane 2), control cells (lane 3), mock transfectants (lane 4), and cells with Vpr expression (lane 5) are shown. Arrow, double-strand breaks. **C**, Rad51 focus formation with Vpr expression. An immunohistochemical analysis was used to detect Rad51 in cells with (right) or without (left) Vpr expression. Bar, 10  $\mu\text{m}$ .

at double-strand break sites (13), were observed with Vpr expression (Fig. 1C). These results indicate that Vpr is responsible for double-strand break formation. The double-strand breaks shown in Fig. 1B were not the result of an apoptotic process as the DNA ladder typically observed in apoptotic cells (14) was not detected (data not shown).

**Vpr has no endonuclease activity.** Next, we studied whether Vpr directly induces double-strand breaks. The recombinant Vpr protein was purified to near homogeneity (Fig. 2A) and the DNA-binding activity of Vpr was examined. As shown in Fig. 2B, purified Vpr bound both ssDNA (lanes 2-6) and dsDNA (lanes 8-12) in an ATP- and  $\text{Mg}^{2+}$ -independent manner (15). Then, we examined whether Vpr has nuclease activity. Superhelical dsDNA containing small amounts of nicked circular dsDNA was incubated with Vpr in the presence of various divalent cations. After the incubation, the proteins were removed and the DNA was examined by

electrophoresis. If Vpr induces a double-strand break or nick, the superhelical dsDNA would give rise to linear or nicked circular forms, producing a different electrophoretic pattern. However, the DNA incubated with Vpr in the absence (*lane 2*) or presence of any divalent cation examined (*lanes 4, 6, 8, and 10*) showed the same migration pattern with control (*lane 1*), indicating that Vpr does not cleave DNA (Fig. 2C). Positive control experiments showed that the DNA was digested by DNaseI with MgCl<sub>2</sub>, MnCl<sub>2</sub>, or CaCl<sub>2</sub> (*lanes 5, 7, and 11*) but not with ZnSO<sub>4</sub> (*lane 9*; Fig. 2C). Therefore, these results indicate that Vpr lacks endonuclease or nicking activity.

**Vpr induces double-strand breaks *in vitro*.** In a second approach, we tested whether purified Vpr induces double-strand breaks in nuclei isolated from HT1080 cells (Fig. 3A). First, we confirmed by a laser confocal microscopy that Vpr localizes in nuclei after incubation *in vitro* (Fig. 3B). The nuclear DNA was then analyzed for double-strand breaks by using PFGE (Fig. 3C). Interestingly, purified Vpr induced double-strand breaks in the DNA of the isolated nuclei (Fig. 3C, *lane 5, arrow*). By contrast, few double-strand breaks were detected without Vpr (Fig. 3C, *lane 4*). Because Vpr alone did not show endonuclease activity (Fig. 2C), these results suggest that Vpr interacts with intrinsic nuclear protein(s), which required for double-strand break formation. To identify candidates for the Vpr-interacting nuclear proteins, we did the Ni-NTA pull-down assay. In this assay, recombinant His<sub>6</sub>-tagged Vpr was incubated with the extract from isolated nuclei and Ni-NTA beads precipitated proteins bound to His<sub>6</sub>-tagged Vpr (Fig. 3D). As shown in Fig. 3D, His<sub>6</sub>-tagged Vpr associated with numerous proteins that were not detected in the control precipitates (*lane 2, asterisks*).

**The DNA-binding activity of Vpr is correlated with double-strand break formation.** The COOH-terminal region of Vpr is arginine rich and is thought to be an important site for DNA binding to Vpr (15). Nuclear magnetic resonance analysis shows that Vpr has three  $\alpha$ -helixes (amino acids 17-33, 38-50, and 56-77)

in solution, whereas the COOH-terminal region from amino acid residues 84 to 96 is disordered (16). This suggests that the deletion of the COOH-terminal 12 amino acid residues does not affect the tertiary structure of Vpr. We purified a Vpr mutant protein lacking the COOH-terminal 12-amino-acid residues (Vpr $\Delta$ C12; Fig. 4A), and examined its DNA-binding activity. Purified Vpr $\Delta$ C12 was significantly defective in both ssDNA- and dsDNA-binding activity compared with wild-type Vpr (Fig. 4B). Interestingly, Vpr $\Delta$ C12 induced double-strand breaks in isolated nuclei but its efficiency was reduced significantly (Fig. 4C, *lane 6*). These results indicate that the DNA-binding ability of Vpr is important for the induction of double-strand breaks by Vpr.

**Discussion**

Here, we present evidence that HIV-1 Vpr induces double-strand breaks. Our data are consistent with previous observations in Vpr-expressing cells: the up-regulation of gene amplification events that are believed to be introduced by broken DNA strands (17) and the activation of activating Rad3-related/ataxia-telangiectasia mutated, followed by the phosphorylation of their downstream substrate, a histone H2A variant, H2AX, and  $\gamma$ -H2AX and BRCA1 focus formation (8). Biochemical analyses using purified Vpr indicated that Vpr alone has no endonuclease activity (Fig. 2C), suggesting that a cellular factor(s), possibly with endonuclease activity, is required for Vpr-dependent double-strand breaks. The factor(s) required for double-strand breaks must preexist in nuclei because double-strand breaks were observed upon incubating a mixture of isolated nuclei and purified Vpr *in vitro* (Fig. 3C). As one possible mechanism, Vpr may recruit a nuclease factor to chromosomal DNA, given that the Vpr-dependent double-strand breaks were correlated with the DNA-binding activity (Figs. 4B and C). Alternatively, Vpr itself may acquire endonuclease activity after modification in the nucleus. Further analyses are necessary to clarify this point.

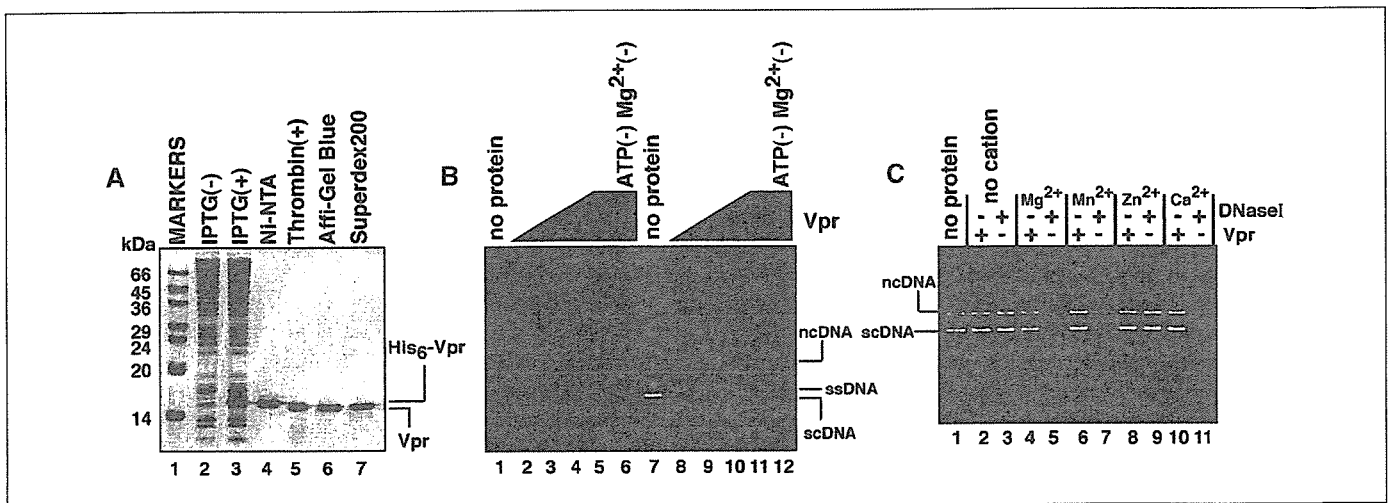


**Figure 2.** The Vpr-DNA interaction *in vitro*. *A*, purification of recombinant Vpr. Proteins from each purification step were analyzed using 16% SDS-PAGE with Coomassie brilliant blue staining. Molecular mass markers (*lane 1*), whole-cell lysates before (*lane 2*) and after (*lane 3*) induction with IPTG, samples from the Ni-NTA fraction (*lane 4*), the fraction after removing the hexahistidine tag (*lane 5*), the Affi-Gel Blue fraction (*lane 6*), and the Superdex 200 fraction (*lane 7*) are shown. *B*, the DNA-binding activity of Vpr.  $\phi$ X174 circular ssDNA (20  $\mu$ mol/L; *lanes 2-6*) and  $\phi$ X174 superhelical dsDNA (*scDNA*; 10  $\mu$ mol/L; *lanes 8-12*) containing a small amount of nicked circular DNA (*ncDNA*) were incubated with Vpr in the presence of 1 mmol/L ATP and 1 mmol/L MgCl<sub>2</sub>. Control experiments without ATP and MgCl<sub>2</sub> (*lanes 6 and 12*) are included. The Vpr concentrations were 1.25  $\mu$ mol/L (*lanes 2 and 8*), 2.5  $\mu$ mol/L (*lanes 3 and 9*), 5  $\mu$ mol/L (*lanes 4 and 10*), and 10  $\mu$ mol/L (*lanes 5, 6, 11, and 12*). *C*, nuclease activity.  $\phi$ X174 *scDNA* (2.5  $\mu$ mol/L) was incubated with Vpr (18.8  $\mu$ mol/L; *lanes 2, 4, 6, 8, and 10*) or DNaseI (*lanes 3, 5, 7, 9, and 11*) in the absence of divalent cation (*lanes 2 and 3*) or in the presence of 5 mmol/L MgCl<sub>2</sub> (*lanes 4 and 5*), 5 mmol/L MnCl<sub>2</sub> (*lanes 6 and 7*), 5 mmol/L ZnSO<sub>4</sub> (*lanes 8 and 9*), or 5 mmol/L CaCl<sub>2</sub> (*lanes 10 and 11*). *Lane 1*, negative control without protein.

In the HIV-1 life cycle, DNA breakage and repair are thought to be essential steps for integrating the double-stranded viral cDNA into the host genome. In this study, we found that Vpr is one molecule responsible for the double-strand breaks that occur upon HIV-1 infection. However, it is also noteworthy that some double-strand breaks were induced in the cells with HIV-1ΔVpr (Fig. 1A, lane 5), suggesting that other viral factors are also involved. It has been shown that integrase activates the ataxia-telangiectasia mutated-dependent pathway (7) and, thus, the double-strand breaks observed with HIV-1ΔVpr infection are probably owing to integrase. For viral integration to occur, the amount of double-strand breaks induced by HIV-1ΔVpr (Fig. 1A, lane 5) may be sufficient, because viral production in peripheral blood mononuclear cells was not alleviated by infection with

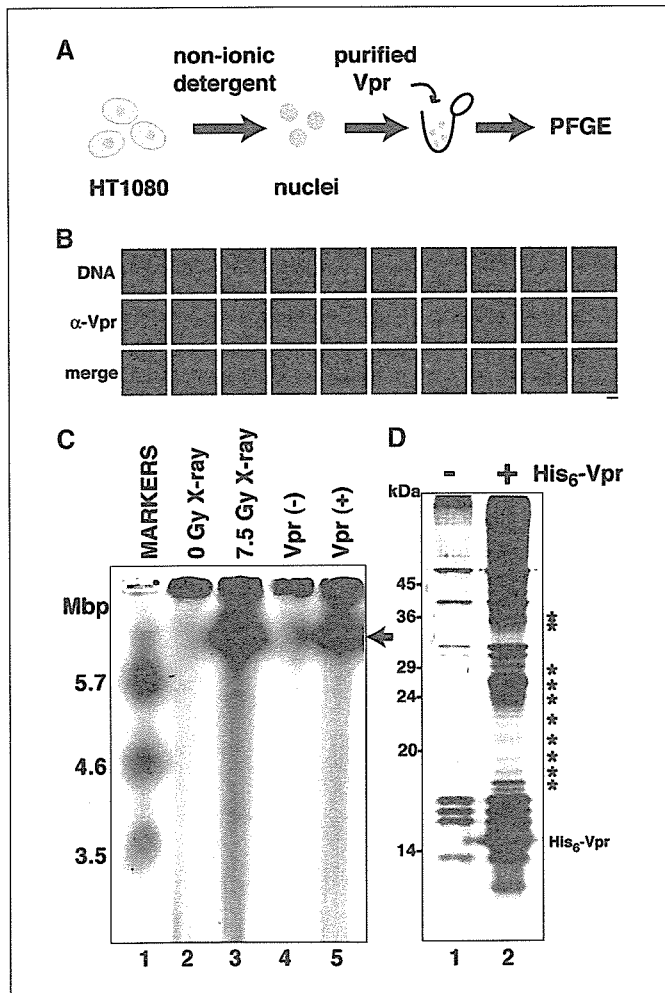


**Figure 3.** Purified Vpr induces double-strand breaks *in vitro*. *A*, a scheme of the protocol used to detect Vpr-induced double-strand breaks in isolated nuclei. *B*, Vpr localization in isolated nuclei. Isolated nuclei from HT1080 after incubation with Vpr were immunostained by  $\alpha$ -Vpr (mAb8D1) and the images were captured by a laser confocal microscopy. The Z-series of optical sections collected at 1  $\mu$ m steps of the cells were presented. Vpr (red; middle), DNA staining by Hoechst (blue; top) and their merged images (bottom) are shown. Without Vpr incubation, any signals by  $\alpha$ -Vpr immunostaining were not detected in isolated nuclei (data not shown). Bar, 10  $\mu$ m. *C*, PFGE analysis of double-strand breaks in isolated nuclei treated with Vpr. Molecular mass markers (lane 1), control cells (lane 2), cells subjected to X-ray irradiation (lane 3), and isolated nuclei without (lane 4) or with 10  $\mu$ mol/L Vpr (lane 5). Arrow, double-strand breaks. *D*, Ni-NTA pull-down assay with His<sub>6</sub>-tagged Vpr on isolated nuclei. Precipitated proteins bound to His<sub>6</sub>-tagged Vpr (lane 2) and the control precipitates (lane 1) are indicated. \*, His<sub>6</sub>-Vpr-specific bands.

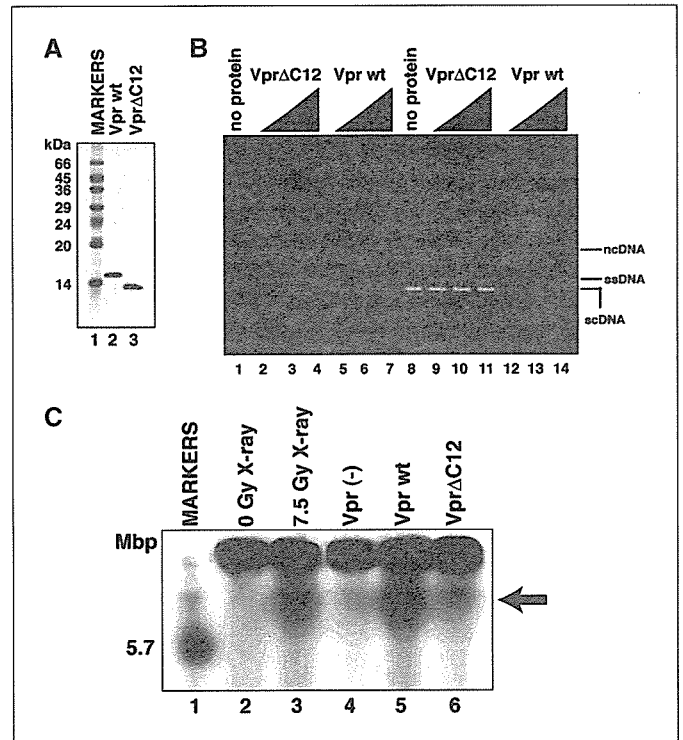


**Figure 4.** DNA-binding and double-strand break formation by Vpr. *A*, purification of VprΔC12. Purified VprΔC12 was analyzed using 16% SDS-PAGE with Coomassie brilliant blue staining. Lane 1, molecular mass markers. Lanes 2 and 3, purified wild-type Vpr and VprΔC12 protein, respectively. *B*, the DNA-binding activity of VprΔC12. The DNA-binding experiments were done using the protocol used to obtain Fig. 2B. The concentrations of VprΔC12 were 2.5  $\mu$ mol/L (lanes 2 and 9), 5  $\mu$ mol/L (lanes 3 and 10), and 10  $\mu$ mol/L (lanes 4 and 11), and those of the wild-type Vpr were 2.5  $\mu$ mol/L (lanes 5 and 12), 5  $\mu$ mol/L (lanes 6 and 13), and 10  $\mu$ mol/L (lanes 7 and 14). Negative controls without protein (lanes 1 and 8) are included. *C*, PFGE analysis of double-strand breaks in isolated nuclei treated with Vpr or VprΔC12. Molecular mass marker (lane 1), cells without (lane 2) or with (lane 3) 7.5 Gy of X-ray irradiation, control nuclei (lane 4), nuclei with Vpr (lane 5), and nuclei with VprΔC12 (lane 6). Vpr was used at 10  $\mu$ mol/L. Arrow, double-strand breaks.

Vpr-deleted HIV-1 (18).<sup>4</sup> Vpr-induced double-strand breaks may be surplus to those required for viral integration (Fig. 1A, lane 6). The resultant DNA damage may reduce the integrity of the host genome.

Recently, DNA damage signaling was observed at an early stage of tumor development, suggesting that the DNA damage response is a mechanism to prevent the progression of pre-neoplastic lesions (5). If DNA repair is not accomplished correctly or is skipped because of unregulated checkpoint controls, the genomic structure would be altered severely (19). The progression of malignant tumors in AIDS-defining cancers is well documented in oncovirus infections (1, 2). If DNA damage increases the probability of neoplasia, Vpr-induced double-strand breaks during the clinical course of AIDS. In addition to AIDS-defining cancers, non-AIDS-defining cancers also occur at a higher incidence and the factor responsible for such oncogenesis is now a critical issue (3, 4). Vpr-induced DNA damage may result in

<sup>4</sup> M. Shimura, unpublished data.

these AIDS-related malignancies. It is essential to explore the molecular mechanism of Vpr-induced double-strand breaks to clarify their role in HIV-1 infection and their effect on the stability of the host cell genome.

## Acknowledgments

Received 9/1/2005; revised 11/16/2005; accepted 11/22/2005.

## References

- Beral V, Peterman T, Berkelman R, Jaffe H. AIDS-associated non-Hodgkin lymphoma. *Lancet* 1991;337:805-9.
- Bellan C, De Falco G, Lazzi S, Leoncini L. Pathologic aspects of AIDS malignancies. *Oncogene* 2003;22:6639-45.
- Wistuba II, Behrens C, Gazdar AF. Pathogenesis of non-AIDS-defining cancers: a review. *AIDS Patient Care STDS* 1999;13:415-26.
- Chiao EY, Krown SE. Update on non-acquired immunodeficiency syndrome-defining malignancies. *Curr Opin Oncol* 2003;15:389-97.
- Bartkova J, Horejsi Z, Koed K, et al. DNA damage response as a candidate anti-cancer barrier in early human tumorigenesis. *Nature* 2005;434:864-70.
- Gorgoulis VG, Vassiliou L-VF, Karakaidos P, et al. Activation of the DNA damage checkpoint and genomic instability in human precancerous lesions. *Nature* 2005;434:907-13.
- Lau A, Swinbank KM, Ahmed PS, et al. Suppression of HIV-1 infection by a small molecule inhibitor of the ATM kinase. *Nat Cell Biol* 2005;7:493-500.
- Zimmerman ES, Chen J, Andersen JL, et al. Human immunodeficiency virus type 1 Vpr-mediated G<sub>2</sub> arrest requires Rad17 and Hus1 and induces nuclear BRCA1 and  $\gamma$ -H2AX focus formation. *Mol Cell Biol* 2004;24:9286-94.
- Shimura M, Tanaka Y, Nakamura S, et al. Micronuclei formation and aneuploidy induced by Vpr, an accessory gene of human immunodeficiency virus type 1. *FASEB J* 1999;13:621-37.
- Adachi A, Gendelman HE, Koenig S, et al. Production of acquired immunodeficiency syndrome-associated retrovirus in human and nonhuman cells transfected with an infectious molecular clone. *J Virol* 1986;59:284-91.
- Tokunaga K, Greenberg ML, Morse MA, Cumming RI, Lyerly HK, Cullen BR. Molecular basis for cell tropism of CXCR4-dependent human immunodeficiency virus type 1 isolates. *J Virol* 2001;75:6776-85.
- Krüger I, Rothkamm K, Löbrich M. Enhanced fidelity for rejoining radiation-induced DNA double-strand breaks in the G<sub>2</sub> phase of Chinese hamster ovary cells. *Nucleic Acids Res* 2004;32:2677-84.
- Haaf T, Golub EI, Reddy G, Radding CM, Ward DC. Nuclear foci of mammalian Rad51 recombination protein in somatic cells after DNA damage and its localization in synaptonemal complexes. *Proc Natl Acad Sci U S A* 1995;92:2298-302.
- Maecker HT, Hedjbeli S, Alzona M, Le PT. Comparison of apoptosis signaling through T cell receptor, fas, and calcium ionophore. *Exp Cell Res* 1996;222:95-102.
- Zhang S, Pointer D, Singer G, Feng Y, Park K, Zhao LJ. Direct binding to nucleic acids by Vpr of human immunodeficiency virus type 1. *Gene* 1998;212:157-66.
- Morellet N, Bouaziz S, Petitjean P, Roques BP. NMR structure of the HIV-1 regulatory protein VPR. *J Mol Biol* 2003;327:215-27.
- Shimura M, Onozuka Y, Yamaguchi T, Hatake K, Takaku F, Ishizaka Y. Micronuclei formation with chromosome breaks and gene amplification caused by Vpr, an accessory gene of human immunodeficiency virus. *Cancer Res* 1999;59:2259-64.
- Kawano Y, Tanaka Y, Misawa N, et al. Mutational analysis of human immunodeficiency virus type 1 (HIV-1) accessory genes: requirement of a site in the nef gene for HIV-1 replication in activated CD4<sup>+</sup> T cells *in vitro* and *in vivo*. *J Virol* 1997;71:8456-66.
- Furuta S, Jiang X, Gu B, Cheng E, Chen PL, Lee WH. Depletion of BRCA1 impairs differentiation but enhances proliferation of mammary epithelial cells. *Proc Natl Acad Sci U S A* 2005;102:9176-81.

ORIGINAL ARTICLE

## HIV-1 Vpr induces ATM-dependent cellular signal with enhanced homologous recombination

C Nakai-Murakami<sup>1</sup>, M Shimura<sup>1</sup>, M Kinomoto<sup>2</sup>, Y Takizawa<sup>3</sup>, K Tokunaga<sup>2</sup>, T Taguchi<sup>1</sup>, S Hoshino<sup>1</sup>, K Miyagawa<sup>4</sup>, T Sata<sup>2</sup>, H Kurumizaka<sup>3</sup>, A Yuo<sup>1</sup> and Y Ishizaka<sup>1</sup>

<sup>1</sup>Departments of Intractable Diseases and Hematology, International Medical Center of Japan, Shinjuku-ku, Tokyo, Japan; <sup>2</sup>Department of Pathology, National Institute of Infectious Diseases, Shinjuku-ku, Tokyo, Japan; <sup>3</sup>Waseda University School of Science and Engineering, Shinjuku-ku, Tokyo, Japan and <sup>4</sup>Section of Radiation Biology, Graduate School of Medicine, The University of Tokyo, Bunkyo-ku, Tokyo, Japan

An ATM-dependent cellular signal, a DNA-damage response, has been shown to be involved during infection of human immunodeficiency virus type-1 (HIV-1), and a high incidence of malignant tumor development has been observed in HIV-1-positive patients. Vpr, an accessory gene product of HIV-1, delays the progression of the cell cycle at the G2/M phase, and ATR–Chk1–Wee-1, another DNA-damage signal, is a proposed cellular pathway responsible for the Vpr-induced cell cycle arrest. In this study, we present evidence that Vpr also activates ATM, and induces expression of  $\gamma$ -H2AX and phosphorylation of Chk2. Strikingly, Vpr was found to stimulate the focus formation of Rad51 and BRCA1, which are involved in repair of DNA double-strand breaks (DSBs) by homologous recombination (HR), and biochemical analysis revealed that Vpr dissociates the interaction of p53 and Rad51 in the chromatin fraction, as observed under irradiation-induced DSBs. Vpr was consistently found to increase the rate of HR in the locus of I-SceI, a rare cutting-enzyme site that had been introduced into the genome. An increase of the HR rate enhanced by Vpr was attenuated by an ATM inhibitor, KU55933, suggesting that Vpr-induced DSBs activate ATM-dependent cellular signal that enhances the intracellular recombination potential. In context with a recent report that KU55933 attenuated the integration of HIV-1 into host genomes, we discuss the possible role of Vpr-induced DSBs in viral integration and also in HIV-1 associated malignancy.

*Oncogene* (2007) 26, 477–486. doi:10.1038/sj.onc.1209831; published online 18 September 2006

**Keywords:** HIV-1; Vpr; DNA double-strand breaks; homologous recombination; Non-AIDS defining malignancies

### Introduction

The induction of a cellular response similar to DNA-damage-sensing signals has been shown during human immunodeficiency virus type-1 (HIV-1) infection (Daniel *et al.*, 1999, 2003, 2004, 2005; Lau *et al.*, 2004). The synthesis of linear HIV-1 DNA in the cytoplasm by reverse transcription and the integration process of HIV-1 DNA into the host genome are thought to be possible triggers for the DNA-damage signals (Lau *et al.*, 2004, 2005). When chromosomal DNA is damaged (DSB; DNA double-strand break), two kinds of kinases (ATM and ATR) are initially activated to exert checkpoint control on cell cycle (Abraham, 2001). When caffeine, which is known to inhibit both ATR and ATM, is administered in conjugation with the viral infection, the integration of viral DNA into the host genome is impaired (Daniel *et al.*, 2005). Additionally, data showing that the recently developed ATM inhibitor KU55933 decreased the copy number of the integrated HIV-1 DNAs strongly suggest that an ATM-dependent signal has a key role in viral transduction (Lau *et al.*, 2005). In addition to the mechanism of viral infection, HIV-1-induced DSBs or their signals have an impact on the approaching AIDS pathogenesis, especially for cancer development. A high incidence of malignant tumors has been reported in AIDS patients (Mayer *et al.*, 1995; Biggar *et al.*, 1996; Straus, 2001), and recent observations have indicated that tumor development is observed even in HIV-1-positive patients who do not show any immunocompromised manifestations (Knowles, 2003). These data suggest that HIV-1 infection is by itself oncogenic (Laurence and Astrin, 1991), but the viral protein responsible for ATM activation during HIV-1 infection has not been well characterized.

Vpr, an accessory gene product of HIV-1, impairs the progression of the cell cycle at G2/M phase (He *et al.*, 1995; Goh *et al.*, 1998). Vpr is thought to inactivate Cdc2, which is a component of maturation-promoting factor, by phosphorylating tyrosine 15 (Bukrinsky and Adzhubei, 1999; Elder *et al.*, 2002). Recent studies have shown that Vpr-induced G2 arrest is attenuated by the introduction of *wee-1* siRNA or deletion of the *wee-1*

Correspondence: Dr Y Ishizaka, Department of Intractable Diseases, International Medical Center of Japan, 1-21-1 Toyama, Shinjuku-ku, Tokyo 162-8655, Japan.

E-mail: zakay@ri.imej.go.jp

Received 22 August 2005; revised 12 May 2006; accepted 12 June 2006; published online 18 September 2006

gene (Yuan *et al.*, 2004). Together with data on a dominant-negative mutant of ATR and its siRNA, ATR–Chk2–Wee-1 as a summarized signal pathway was postulated to be responsible for the Vpr-induced G2 arrest (Roshal *et al.*, 2003; Yuan *et al.*, 2004; Zimmerman *et al.*, 2004). As an earlier study demonstrated that ATM was not important for Vpr-induced G2 arrest (Bartz *et al.*, 1996), there have been no reports that describe the activation of ATM under Vpr expression. To investigate the Vpr-induced cell cycle abnormalities, we established a MIT-23 cell line, in which Vpr expression is tightly regulated by a tetracycline promoter (Shimura *et al.*, 1999b). We found that the continuous expression of Vpr induced the formation of TUNEL-positive micronuclei and increased the rate of gene amplification (Shimura *et al.*, 1999a), implying that Vpr induces DSBs. Through an analysis with a pulse-field gel electrophoresis on HIV-1 infected cells, we recently detected an altered migration pattern of high-molecular-weight genomic DNA (Tachiwana *et al.*, 2006), also implying that Vpr induces DSBs. Thus, it is now important to clarify whether a cellular response dependent on ATM, a kinase activated selectively by DSBs (O'Connell *et al.*, 2000; Khanna *et al.*, 2001; Shiloh, 2001), is really induced by Vpr, and if so, we need to determine whether Vpr is the major viral protein responsible for ATM activation.

DNA damage is induced by reactive oxygen species, ionizing radiation, and chemicals (Abraham, 2001), and are repaired by homologous recombination (HR) or nonhomologous DNA end-joining (NHEJ) pathways (Khanna and Jackson, 2001; van Gent *et al.*, 2001). Once a DSB is generated, a 3' single-stranded DNA tail is processed, where replication protein A (RPA) and Rad51, an eukaryotic homologue of the bacterial DNA strand exchange protein RecA (Cromie *et al.*, 2001; West, 2003), accumulate. It was shown that p53 and BRCA2 phosphorylated at serine 3291 bind Rad51 and suppress its HR activity (Dong *et al.*, 2003; Linke *et al.*, 2003; Yoon *et al.*, 2004). Functional BRCA1 and 2 are required when DSBs occur; otherwise, genomic instability is induced, as observed in cancer-prone individuals with mutations of these genes (van Gent *et al.*, 2001; Dong *et al.*, 2003).

In this report, we first show that Vpr induced an ATM-dependent cellular signal. The cellular response under Vpr expression was similar to that caused by X-ray irradiation involving BRCA1, RPA and Rad51. We next demonstrate that Vpr increased the frequency of HR in an ATM-dependent manner. Data support the idea that Vpr induces DSBs. The possible role of Vpr in viral infection and in HIV-1-associated malignant tumor development is discussed.

## Results

### DSB-induced cellular signals by Vpr

Initially, we examined whether DSB-dependent cellular signals were induced by HIV-1 infection. HT1080 cells

were infected with viruses without (R<sup>-</sup>) or with wild-type *vpr* (R<sup>+</sup>), and an immunohistochemical analysis was performed. As shown in Figure 1a,  $\gamma$ -H2AX accumulated after infection with the R<sup>+</sup> virus (right panels) but not with the R<sup>-</sup> virus (Figure 1a, middle panels). Western blot analysis demonstrated a high-level expression of  $\gamma$ -H2AX with the phosphorylation of p53 in cells infected with the R<sup>+</sup> virus (Figure 1b, lanes 4 and 5). Viral concentrations of 50 and 100 ng/ml of p24 were sufficient for the induction of  $\gamma$ -H2AX. In contrast, the R<sup>-</sup> virus did not induce p53 phosphorylation, although it slightly increased p53 expression (Figure 1b, lanes 2 and 3).

To characterize the intracellular signals specifically induced by Vpr, we used MIT-23 cells, in which *vpr* mRNA expression was tightly regulated by the tetracycline promoter (Shimura *et al.*, 1999b). In MIT-23 cells, Vpr expression was observed in 48 h after treatment of 3  $\mu$ g/ml of doxycycline (DOX) (Figure 2a). Under such conditions, we observed focus formation of ATM phosphorylated at serine 1981 (ATM-p) (Figure 2b, upper panels) and  $\gamma$ -H2AX (lower panels). In contrast, focus formation of these molecules was not observed in MIT-23 cells without DOX treatment (left panels). Additionally, we did not detect focus formation of

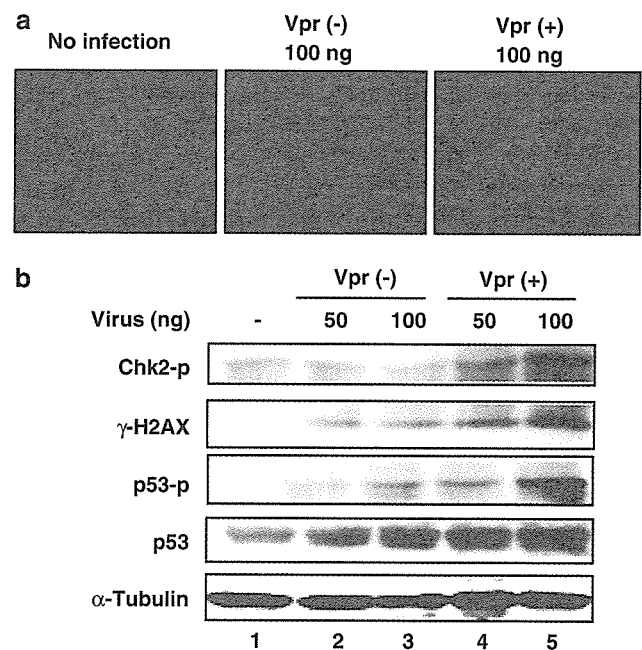


**Figure 1** Activation of DSB-induced signaling. (a) Focus formation of  $\gamma$ -H2AX in cells infected with R<sup>-</sup> or R<sup>+</sup> virus. HT1080 cells were infected with R<sup>-</sup> or R<sup>+</sup> virus at the concentration of 100 ng/ml of p24 gag protein. After 48 h of infection, the cells were stained with specific antibody against  $\gamma$ -H2AX. The signals for  $\gamma$ -H2AX are shown as red spots in the nucleus (blue). (b) Western blot analysis of proteins involved in the DSB-induced signal pathway. Cell lysates of virus-infected and control cells after 48 h were subjected to analysis. Control cells (lane 1), cells infected with R<sup>-</sup> virus (lanes 2 and 3), and cells infected with R<sup>+</sup> virus (lanes 4 and 5) are shown. Two doses of viruses at the concentration of 50 (lanes 2 and 4) and 100 ng/ml of p24 gag protein (lanes 3 and 5) were used.  $\alpha$ -Tubulin indicates that the amounts of loaded proteins are not significantly different.



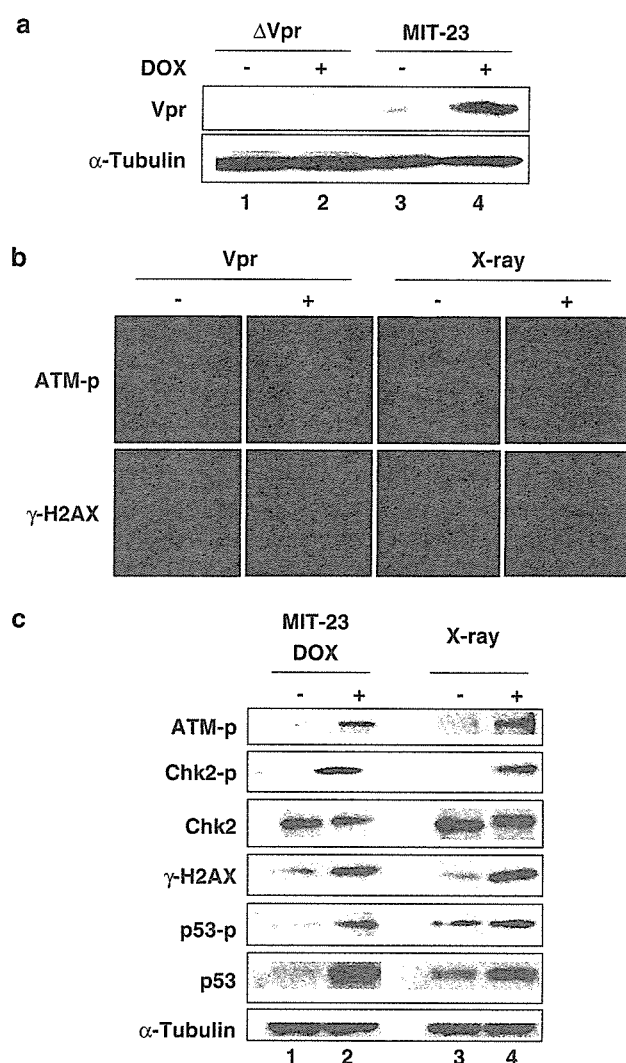


**Figure 2** Activation of DSB-induced cellular signaling. (a) Expression profiles of Vpr in MIT-23 cells. Vpr expression was induced in 48 h with 3  $\mu$ g/ml DOX in MIT-23 cells. The Vpr expression level in MIT-23 cells was analysed by Western blotting with the Vpr-specific antibody 8D1. (b) Focus formation of phosphorylation of ATM (ATM-p) and  $\gamma$ -H2AX following Vpr expression. The cells were stained with specific antibodies against ATM-p and  $\gamma$ -H2AX. The signals for ATM-p and  $\gamma$ -H2AX are depicted as red spots in the nucleus (blue). (c) Western blot analysis of proteins involved in the DSB-induced signal pathway. Cell lysates of MIT-23 cells (lanes 1 and 2) were subjected to analysis. As a positive control, HT1080 cells were irradiated at 7.5 Gy, collected after 30 min, and subjected to analysis.

ATM-p or  $\gamma$ -H2AX in DOX-treated  $\Delta$ Vpr cells, in which only the *vpr* gene was eliminated from vectors that were utilized for the establishment of MIT-23 cells (data not shown). Western blot analysis also detected that DNA-damage-sensing signals were induced by Vpr expression (Figure 2c). Interestingly, Chk2, a substrate of ATM, was highly phosphorylated at threonine 68 by Vpr expression (Figure 2c, lane 2). Additionally, p53 expression as well as its phosphorylation also increased as a downstream response of these molecules. Consistent with the previous

report showing that Chk1, a substrate of ATR, is activated by Vpr (Roshal *et al.*, 2003), we observed the presence of the slowly migrating band of Chk1 as its phosphorylated form under Vpr expression (data not shown).

To compare the Vpr-induced DSB-dependent signals with those by X-ray irradiation, HT1080 cells were irradiated with 7.5 Gy of X-rays, and the evoked signals were analysed. As shown in Figure 2b (right panels), X-ray-induced DSBs generated focus formation of ATM-p (Figure 2b, upper panel) and  $\gamma$ -H2AX (lower panel). Additionally, Western blot analysis clearly demonstrated the phosphorylation of both Chk2 and p53 (lane 3 and 4). Data suggest that Vpr-induced DNA-damage signals are quite similar to those triggered by a well-characterized DSB inducer.

#### *Mobilization of cellular factors that are involved in repair of DSBs*

To further characterize the molecules activated as a cellular response to Vpr-induced DSBs, we investigated BRCA1, RPA and Rad51 mobilized for repair of DSBs (West, 2003). As shown in Figure 3, the immunohistochemical analysis carried out under Vpr expression clearly detected focus formation of these molecules (Figure 3). In contrast, control cells did not show remarkable modification of these molecules. Again, X-ray irradiation also induced the same modification of the molecules (Figure 3, right panels).

It has been proposed that during the DSB repair process, Rad51 is released from a complex of p53 and becomes competent for HR (Linke *et al.*, 2003; Bertrand *et al.*, 2004). To address this possibility, we compared the physical association of Rad51 and p53 in the insoluble chromatin fraction before and after the induction of Vpr expression. The interaction of these molecules was eliminated following Vpr expression (Figure 4a, lanes 3 and 4; arrow). The level of the complex formation of p53 and Rad51 decreased by 35% compared to the control. This finding is reproducibly observed, implying the possibility that Vpr binds either Rad51 or p53 and ceases their interaction. We examined the direct interaction of Vpr and Rad51 by using recombinant proteins, but did not obtain positive results (data not shown). As it has been shown that Vpr does not interact with p53 (Sawaya *et al.*, 1998), the mechanism of dissociation of p53 and Rad51 in Vpr-expressing cells remains to be clarified.

We also compared this molecular change with that induced by X-ray irradiation. HT1080 cells were irradiated, and the subsequent change of the interaction of Rad51 and p53 was examined. As observed in Figure 4a, the interaction between Rad51 and p53 in the insoluble chromatin fraction was also abolished (Figure 4b, compare lanes 3 and 4, arrow). Data suggest that Vpr modifies Rad51 in the same way as X-ray irradiation.

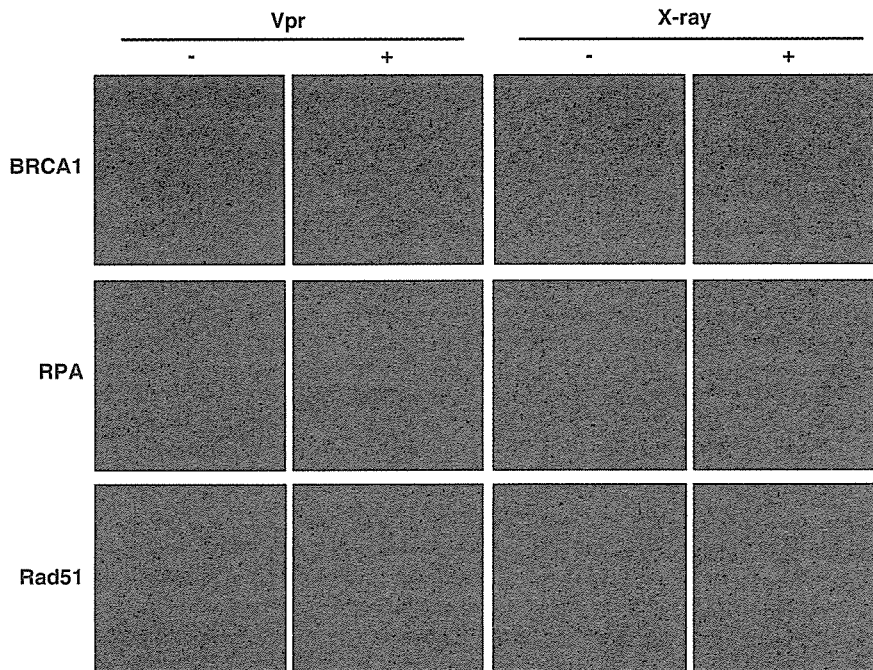


**Figure 3** Involvement of BRCA1, RPA and Rad51 in Vpr-induced signaling. MIT-23 cells were cultured in the presence or absence of 3  $\mu\text{g/ml}$  DOX for 48 h. Focus formations of BRCA1, RPA and Rad51 during Vpr expression are shown. These signals are visualized as red spots in the nucleus (blue).

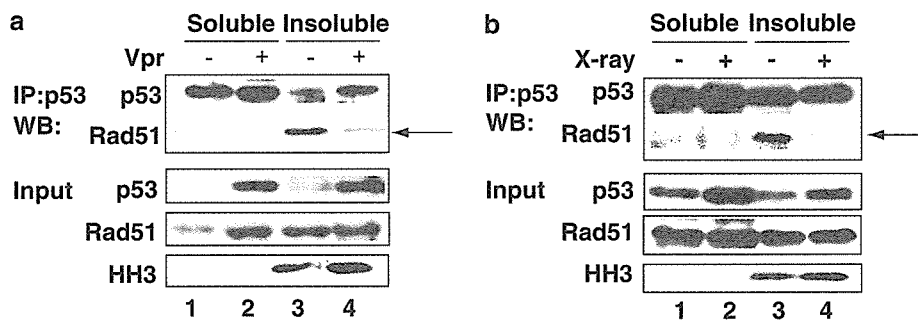


**Figure 4** Dissociated interaction of p53 and Rad51 in a chromatin fraction during Vpr expression. The lysates of the soluble (lanes 1 and 2) and insoluble chromatin fractions (lanes 3 and 4) subjected to analysis. Proteins that were immunoprecipitated (IP) with the anti-p53 antibody ( $\alpha\text{p53}$ ) were analysed by Western blot analysis (WB) with the  $\alpha\text{p53}$  and  $\alpha\text{Rad51}$  antibodies, respectively. Input lysates were also analysed by the same antibodies and  $\alpha\text{histone H3}$  (HH3). The cell lysate with (lanes 2 and 4) or without (lanes 1 and 3) Vpr expression are shown (a). The same analysis was performed on X-ray irradiated cells (b). Arrowheads indicate Rad51 recovered by  $\alpha\text{p53}$  antibody.

#### Increased rate of HR by Vpr

DSBs must be correctly repaired, or genome integrity cannot be maintained (West, 2003). As Vpr induces DSBs and cellular factors such as Rad51 and BRCA1 are mobilized under Vpr expression, we hypothesized that the rate of HR increased in Vpr-expressing cells. To measure the rate of HR, we first utilized a system invented by Slebos and Taylor (2001) that could monitor extrachromosomal recombination within a plasmid DNA (pBHRF). pBHRF contains a truncated EBFP cassette, which forms a functional EGFP following intramolecular HR (Slebos and Taylor, 2001). We co-transfected HT1080 with pBHRF and a plasmid DNA encoding Vpr and examined the effects of Vpr on HR.

After 72 h of transfection, the EGFP- and EBFP-positive cells were counted by flow cytometry (Figure 5a, regions a and b, respectively). Then, the frequency of HR was calculated as a ratio of number of cells positive for EGFP and EBFP. It increased about 2.5-fold by co-transfection of a plasmid encoding Vpr. Vpr-induced enhancement of HR was reproducibly observed ( $P < 0.05$ ), and the representative results are shown in Figure 5b.

Although the experiments with pBHRF strongly suggested that Vpr increases HR, it has been demonstrated that an extrachromosomal HR does not correlate with intrachromosomal HR. Waldman and Liskay (1987) clearly demonstrated that the frequency of

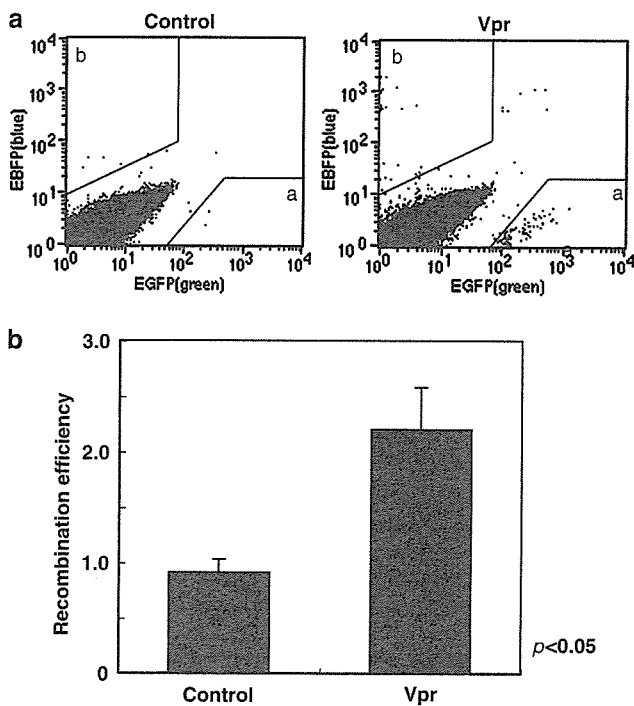


**Figure 5** Increased rate of extrachromosomal HR by Vpr. (a) A representative result of three independent experiments with pBHRF. HT1080 cells were co-transfected with pBHRF and pDNA3.1/Vpr (see Materials and methods section). The cells were subjected to analysis by flow cytometry after 72 h. Regions a and b were tentatively determined in a control sample. These indicate the areas where cells positive for EGFP (region a) or EBFP (region b) were not present in untreated samples. After treatment cell numbers in these areas were counted and compared. (b) Increase of GFP-positive cells by Vpr. The ratio of GFP-positive cells to BFP-positive cells, which are indicative of HR frequencies (Slebos and Taylor, 2001), were counted. Each sample was analysed twice in triplicate; bars  $\pm$  s.d.

extrachromosomal and intrachromosomal recombination rates are differentially influenced by the mismatch of the nucleotides. To measure the rate of intrachromosomal HR under Vpr expression correctly, we prepared stable transfectants derived from HT1080 cells that had been introduced with pDR-GFP. pDR-GFP is a reporter construct that will generate an intact EGFP gene by gene conversion after digestion with a rare cutting enzyme, I-SceI (Pierce *et al.*, 1999). We obtained two independent transfectants, HT/DR-GFP-1 and -2, that possessed an integrated exogenous plasmid DNA competent for a short tract gene conversion (Supplementary information 1a) (Pierce *et al.*, 1999). Then, HT/DR-GFP cells were infected with adenoviruses of either Ad $\beta$ gal or Ad-SceI-NG and subjected to analysis of GFP-positive cells after 72 h. After infection with Ad-SceI-NG, both clones gave increased numbers of GFP-positive cells (about 0.5%) (Supplementary information 1b and c). In contrast, Ad $\beta$ gal, control adenovirus, induced very few cells positive for GFP (<0.1%) (Supplementary information 1b and c).

We then examined the influence of Vpr on the rate of HR. First, we introduced a plasmid DNA encoding Vpr or its control plasmid DNA, but it was not possible to

assess the effects of Vpr correctly because transfection of plasmid DNA by itself influenced the rate of HR (data not shown). It has been well reported that Vpr enters cells and expresses its biological activity when added to the cell culture (Jenkins *et al.*, 1998; Henklein *et al.*, 2000; Huang *et al.*, 2000; Taguchi *et al.*, 2004). These observations encouraged us to perform the experiments by adding Vpr to cells exogenously with subsequent measurement of GFP-positive cells. We prepared a recombinant Vpr (rVpr) (Hoshino *et al.*, submitted), and we first checked whether exogenously added rVpr induces DSB-triggered cellular response. rVpr (50 ng/ml; 3.7 nM) added to the medium induced DSB-dependent signals (Figure 6a), whereas glutathione S transferase (GST), an irrelevant recombinant protein that was expressed in bacteria and purified, did not (right panels). Interestingly, the addition of the ATM inhibitor KU55937 abolished rVpr-induced focus formation of ATM-p and  $\gamma$ -H2AX (Figure 6a).

When rVpr was added to HT/DR-GFP-1 (clone-1), HR especially after infection with Ad-SceI-NG-infected was definitely enhanced (about 1.5%), whereas it was not remarkably changed by the addition of GST (Figure 6b and c, left panel). The difference in GFP-positive numbers after treatment with rVpr and GST was statistically significant ( $P < 0.01$ ). As more striking evidence, the addition of KU55933 significantly attenuated the increased number of GFP-positive cells caused by rVpr (Figure 6c, right panel) ( $P < 0.01$ ). Data indicate that ATM is a critical molecule for the Vpr-induced enhancement of HR.

## Discussion

### Vpr induces DSBs and enhances HR

In this study, we showed that Vpr activates the ATM-dependent signal pathway involving Chk2 phosphorylation with focus formation of Rad51, BRCA1 and  $\gamma$ -H2AX. We previously reported that Vpr increases the rate of gene amplification (Shimura *et al.*, 1999a), and a subsequent analysis by fluorescence *in situ* hybridization of amplified DNA suggested that a bridge-breakage fusion cycle, possibly triggered by DSBs (Ishizaka *et al.*, 1995), was a relevant mode of Vpr-induced gene amplification. Data shown in the present study well supports our expectation that Vpr enhances gene amplification by causing DSBs (Shimura *et al.*, 1999a).

We observed that the frequency of HR increased in response to Vpr. We examined the rate of HR by two systems measuring extrachromosomal recombination (Slebos and Taylor, 2001) and intrachromosomal recombination (Pierce *et al.*, 1999). Both systems detect cells that are positive for GFP generated by gene conversion. Although it has been claimed that these two modes of HR do not always equally detect cellular recombinogenic conditions, our present data revealed that both systems detected the effects of Vpr on HR. It is interesting to note that the intrachromosomal recombination system used in the current study detects HR at

the specific site in the genome, where DSB is induced by expressing I-SceI, a rare-cutting enzyme (Anglana and Bacchetti, 1999). We used two cell lines, both of which contained reporter constructs that were competent for a short tract gene conversion (Pierce *et al.*, 1999; Supplementary information 1), and we reproducibly detected enhancement of HR after treatment with Vpr. Data suggest that Vpr has an indirect effect on HR,

indicating that DBSs at one locus contribute to trans-activation of HR at a different site.

In response to Vpr-induced DSBs, BRCA1 and RPA accumulated as foci (Figure 2b), and the association of Rad51 and p53 in the chromatin fraction was eliminated (Figure 3a and b). It has been reported that p53 associates with several proteins including BLM, BRCA1, BRCA2, Rad52 and RPA (Yamaguchi-Iwai

